Partial volume segmentation using super-resolution, structure maps and multi-scale processing

J. P. Withers[1], M. E. Bastin[2], and A. J. Storkey[1]

[1]School of Informatics, University of Edinburgh, Edinburgh, Midlothian, United Kingdom, [2]Medical Physics, University of Edinburgh, Edinburgh, Midlothian, United Kingdom

Introduction: The correct segmentation of a MRI brain volume into its constituent tissue types, such as white matter (WM), gray matter (GM), cerebrospinal fluid (CSF) and background/blood (BG), is of considerable importance to its subsequent analysis. However, manual segmentation is slow, displays high inter-observer variability, and frequently assumes that voxels can always be assigned to a single pure tissue class. Automatic segmentation algorithms can be faster and more consistent, but there is a trade-off between providing robustness to noise and recognizing fine structures. In addition, there may be restrictive assumptions on the presence of tissue mixtures, such as confining them to tissue region boundaries, and prior information from average brain tissue maps may be required. Unfortunately these maps may not represent the target volume well, nor can they match unique components of brain structure such as blood vessels or cortical sulci. Here we present methods for the detection of these thin structures which allows them to be processed at a different scale to the rest of the volume. A super-resolution process further enhances these features, smoothes pure tissue regions and reduces aliasing at tissue boundaries. In addition, knowing the presence of blood vessels and sulci provides strong priors for BG and CSF tissue types.

Methods: An extension of work by Frangi *et al.* [1] exploits the contrast of dark blood vessels in PD-weighted volumes and bright cortical sulci in T_2-weighted volumes in order to detect these fine features. By examining the signs of the eigenvalues of the Hessian matrix in MRI data and choosing an appropriate threshold for the difference in their magnitude, dark or bright tube-like structures can be mapped without including noise. Salvado *et al.* [2] have developed a super-resolution process using reverse diffusion to minimize aliasing at tissue boundaries. MRI-specific constraints allow intensity flow only inside voxels, not between them, so the intensity of the image is preserved and noisy voxels do not substantially impact the super-resolved image. Local rank-order limits on the possible flow create a trade-off between robustness to noise and the amount of aliasing reduction. Since we now know the locations of fine structure in the volume, this allows for smaller and tighter smoothing kernels with more extreme flow limits to be applied in these areas.

The main segmentation method extends the approach of FAST [3] to allow a minimal range of discrete tissue mixture states anywhere in the volume. The distance of the decision boundary between the few pure and mix states as well as the aliasing reduction effects of the super-resolution process both promote label homogeneity in the presence of noise. In regions determined as possessing CSF or BG structures a penalty to the likelihood is imposed for states containing none of these tissues. A distance metric for mixture states is built into the neighborhood interaction term, and the size and strength profile of the local label interaction filter is scalable: it can be increased to deal with the greater resolution of super-resolved images for the purposes of noise reduction, and reduced to preserve fine structures. Finally, the maximization-step update equations of Li *et al.* [4] are employed to re-estimate the pure class parameters based on the mixture segmentation.

BrainWeb [5] synthetic images were employed for testing the methods against a ground truth result. In addition, a dual-echo proton density (PD) and T_2-weighted FSE dataset was acquired from a volunteer to obtain qualitative feedback. The MRI data were pre-processed to remove bias field effects and non-brain tissue using BSE and BFC [6].

Results: Only 2% of voxels flagged as containing CSF had none actually present (Fig 1A&1B), using tube-like structure detection on a BrainWeb T_2-weighted volume. A substantial amount was successfully detected, but large bodies of CSF were not flagged as the method only worked at a single scale. The level of error was found to scale with the amount of noise (Fig 1B). The method was also successfully applied to real MRI datasets (Fig 1C), though the detection threshold was increased slightly to exclude noise.

After removing non-brain voxels from analysis, the mean segmentation error in terms of absolute distance from the BrainWeb generating map ground truth was 0.134 ± 0.211, and 91.8% of voxels were labeled with the correct constituent tissue types (Table 1). CSF displayed the best labeling, with the majority of the mean 0.0258 ± 0.0683 error stemming from slight differences in the quantification of partial volume on tissue boundaries. The GM segmentation was the furthest from the ground truth with a 0.0644 ± 0.102 error, where some interfaces between CSF and GM were poorly quantified and thin areas of GM were sometimes mislabeled. The real brain images displayed good label homogeneity in WM regions (Fig 2A&2B) and CSF again displayed the best labeling. At the edges of the cortex too many partial volume voxels were labeled (Fig 2C&2D), but deep gray matter structures were clearly visible. The processing took 17 minutes on an Intel Core2 2.4GHz workstation with 4GB RAM.

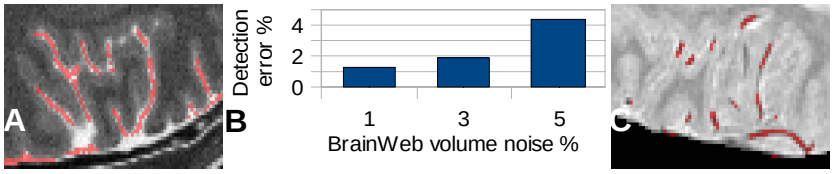

Figure 1: Vessel detection quality; tube-like structures detected are marked in red. (**A**) Close-up of T_2 BrainWeb slice (3% noise) with CSF marked. (**B**) Quantification of detected CSF voxels with 0% actual CSF in 5 T_2 BrainWeb slices. The detection threshold τ was held constant at 0.1. N(1%) = 8326, N(3%) = 8215, N(5%) = 8076. (**C**) Close-up of PD-weighted real MRI slice with BG marked.

	All	*WM*	*GM*	*CSF*
Distance from ground truth	0.134 ±0.211	0.0432 ±0.0934	0.0644 ±0.102	0.0258 ±0.0683
Correctness of mix classes estimation	91.80%	92.30%	93.40%	93.80%

Table 1: Accuracy of the segmentation method against the ground truth of the BrainWeb generating maps. The mean absolute distance between the estimated mix and the ground truth is measured (with an optimum of 0 and worst case of 2), as well as a percentage measure of the correct presence of the component tissue types (correctness). The results are taken over brain voxels in 3 central slices of PD- and T_2-weighted BrainWeb volumes with 3% noise levels relative to the maximum intensity. Values are ± SD, N = 58140.

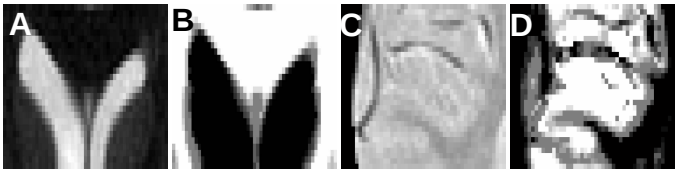

Figure 2: Segmentation quality in close-ups of real brain MRI. (**A**) Close-up of the top of the ventricles (T_2-weighted slice shown). (**B**) WM tissue contribution map. (**C**) Close-up of temporal cortex (PD-weighted slice shown). (**D**) GM tissue contribution map.

Discussion: The methods presented are able to create an automatic partial volume segmentation of an MRI volume, without any restrictions on the presence of partial volume voxels nor any prior knowledge from average brain maps. The preservation of fine structures in the image is comparable to segmentation methods with less aggressive homogeneity constraints, such as Fuzzy C-Means [7], but with improved robustness to noise. While the detection of tube-like structures is an active area of research in several fields, to our knowledge this feature-based prior has not been employed in the segmentation of brain volumes. Several avenues exist for further improvement of the detection method, including multi-scale processing to find larger regions, more detailed analysis of the Hessian matrix, and the development of geometric priors and morphological operators to better describe blood vessels and sulci. The segmentation result can also be improved, especially in deep GM, by re-classification of large regions of partial volume voxels into a greater range of mixture states.

References: [1] Frangi A, et al. *Lecture Notes in Computer Science* 1998;**1496**:130-137. [2] Salvado O, Hillenbrand C & Wilson D. *Proc of the SPIE* 2005;**5747**:625-633. [3] Zhang Y, Brady M & Smith S. *IEEE TMI* 2001;**20**:45-57. [4] X Li, et al. *IEEE Nuclear Science Symposium Conference Record* 2003;**5**:3176-3180. [5] Cocosco C, et al. *Neuroimage* 1997;**5**:S425. [6] Shattuck D, et al. *NeuroImage* 2001;**13**:856-876. [7] Ahmed M, et al. *IEEE TMI* 2002;**21**:193-200.